Chapter 7
Combustion Products from Fires

Abstract Knowledge of the different species produced during fires is of great importance for estimating the toxicity of the fire gases. In this chapter the main combustion products from different types of fires are presented. This includes carbon monoxide (CO), carbon dioxide (CO_2), hydrogen chloride (HCl), sulphur dioxide (SO_2), volatile organic compounds (VOCs), polycyclic aromatic hydrocarbons (PAHs), polychlorinated dibenzo-p-dioxins and dibenzofurans (PCDDs/PCDFs), total amount of hydrocarbons (THC) and soot/smoke, but yields also for some other species are presented. Results from measurement during fire tests in vehicles and tunnels are summarized and discussed. The importance of the ventilation conditions (equivalence ratio) on the productions of different species is described and relations for different yields and ratios are given and discussed.

Keywords Combustion products · Carbon monoxide · Carbon dioxide · Smoke · Ventilation conditions · Equivalence ratio · Yield · Species

7.1 Introduction

The reason for fatalities in fires is most often due to inhalation of fire gases. In several of the catastrophic fires presented in Chap. 1, people were found dead in their cars. Increased temperature can, however, affect both the physical health and the capacity to escape. Among the fire effluents, carbon monoxide (CO) is seen to be the most important component responsible for causing fatalities, even if the effect of hydrogen cyanide (HCN) has been much discussed during recent years [1–4]. In a comprehensive review, Nelson showed that even if high blood concentrations of HCN were found in fire victims, most fatalities can be explained by the CO concentration [5]. Furthermore, carbon dioxide (CO_2) has an important effect on tenability, not only by being toxic at high levels, but mostly by increasing the uptake of other fire gases, for example, CO, due to increasing the breathing rate.

Even if fire gases do not always lead to fatalities, sublethal effects, for example, incapacitation, reduced egress speed, reduced motor capability, decreased mental acuity, and visual obscuration are also important [6]. Further, many effluents can

H. Ingason et al., *Tunnel Fire Dynamics,* DOI 10.1007/978-1-4939-2199-7_7

cause long-term or chronic effects, which is of particular importance for firefighters and rescue personal.

Another issue becoming increasingly important in the context of fire emissions is the effect on the environment and emissions which may pose potentially long-term hazards to health. Even if they have not typically been considered to be central issues for fires in tunnels, this is an issue related to all fires. More detailed aspects of toxicity and tenability are presented and discussed in Chap. 15.

In the design of tunnel ventilation, even the ventilation of gases in a nonfire situation is an important issue. That is in most cases the main reason why ventilation systems are installed in tunnels in the first place. Traditionally, the concentration of CO exhausted from the vehicles has been used to design the ventilation systems, but because of the development of new vehicles and new fuels, the emissions of CO has decreased significantly [7]. For this reason, concentrations of other species, for examples, NO_x (most often with a guideline concentration for NO_2) have also been included in the design of the ventilation system.

This chapter discusses what species are produced during a fire and how different parameters and conditions, that is, the ventilation conditions and temperature, affect the production. Not only acute toxic species are included in the discussions, but also the production of species interesting for other reasons.

7.2 Combustion and Fire Chemistry

Fire is a field of combustion, often referred to as uncontrolled combustion. Combustion involves a large number of elementary (intermediate) reactions. These different reactions (steps) can be grouped depending on whether or not free radicals are formed or consumed in the reactions. Free radicals are atoms, molecules, or ions that have unpaired valence electrons or an open electron shell and, therefore, in most situations are highly reactive. The following types of reaction can be identified, here exemplified with reactions in the hydrogen–oxygen system [8, 9]:

1. Chain initiating step:

The reaction chain starts with an initiating step where free radicals are formed.

Free radicals (in the reactions marked with a dot) are produced from stable species, for example:

$$H_2 + O_2 = 2\,OH\cdot \tag{7.1}$$

2. Chain propagating (or carrying) steps

A radical reacts with stable species to form a new free radical, for example:

$$OH\cdot + H_2 = H_2O + H\cdot \tag{7.2}$$

3. Chain branching step:

A free radical reacts with a stable species forming two free radicals, that is, the number of free radicals increases, for example:

$$\mathrm{H\cdot} + \mathrm{O_2} = \mathrm{OH\cdot} + \mathrm{O\cdot} \tag{7.3}$$

4. Chain terminating step

Free radicals react to form stable species, that is, free radicals are "consumed", *for example,*

$$2\,\mathrm{H\cdot} = \mathrm{H_2} \tag{7.4}$$

Even for relatively simple fuels, there are a large number of elementary reactions, often combined in complex reaction schemes. It is not the aim of this chapter to in detail discuss these elementary reactions. Instead the simplified "global" reaction will be discussed and how this reaction is affected by the fire conditions and how these conditions influences what species are produced during a fire.

If a hydrocarbon fuel, with or without oxygen, is involved in the fire and complete combustion is assumed the following global reaction can be written:

$$C_aH_bO_c + \left(a + \frac{b}{4} - \frac{c}{2}\right)(O_2 + 3.76N_2) \rightarrow aCO_2 + \frac{b}{2}H_2O + \left(a + \frac{b}{4} - \frac{c}{2}\right)3.76N_2 \tag{7.5}$$

In a combustion reaction energy is also released and from the global reaction the heat of combustion can be derived (for example, by assuming all H_2O being released in gas phase). The fuel can also contain other elements (N, S, Cl, Br, etc.). In those cases it must either be known or assumed what species are formed.

In Sect. 7.5, the effect of ventilation conditions on the production of different species is presented. For this often the equivalence ratio, ϕ, is used. To calculate this parameter, the ideal reaction stoichiometric air to fuel ratio for complete combustion, r, can be used. This parameter is defined by:

$$1\,\mathrm{kg\ fuel} + \mathrm{r\,kg\ air} \rightarrow (1 + \mathrm{r})\,\mathrm{kg\ products} \tag{7.6}$$

For complete combustion it is assumed that there is exactly enough air for the fuel to completely (ideally) react and produce CO_2 and H_2O as described by Eq. (7.5). These conditions are called stoichiometric and the stoichiometric coefficient, r, can be calculated (using the notation in Eq. (7.5)) as[1]:

$$r = \frac{(1+3.76)M_{air}\left[a+(b/4)-(c/2)\right]}{M_C\cdot a + M_H\cdot b + M_O\cdot c} \approx \frac{137.9\left[a+(b/4)-(c/2)\right]}{12\cdot a + b + 16\cdot c} \tag{7.7}$$

---

[1] See also Eq. (2.13).

Table 7.1 Molecular weight of selected species and concentration of main components in air

Species	Molecular weight	Concentration in air (vol-%)	Reference
Carbon dioxide, CO_2	44.010	0.04	[10, 11]
Carbon monoxide, CO	28.010	–	[10]
Carbon, C	12.011	–	[10]
Oxygen, O_2	31.999	20.946	[10, 12]
Nitrogen, N_2	28.013	78.084	[10, 12]
Argon, Ar	39.948	0.934	[12, 13]
Air (dry)[a]	28.967		

[a] Based on the concentrations and molecular weights given in the table

where the molecular weight, M_i, for air and different atoms are given in Table 7.1.

Note that r in some literature is defined as the stoichiometric fuel to air ratio.

The equivalence ratio, ϕ, which is the quotient between the actual fuel/air ratio and the stoichiometric fuel/air ratio, is here defined as[2]:

$$\phi = \frac{\dot{m}_f / \dot{m}_a}{\left(\dot{m}_f / \dot{m}_a\right)_{stoich.}} = \frac{\dot{m}_f \cdot r}{\dot{m}_a} \tag{7.8}$$

where

$\phi = 1$ stoichiometric combustion
$\phi < 1$ well-ventilated combustion
$\phi > 1$ under ventilated combustion

where $\dot{m}_f$ is the mass loss rate of the fuel (kg/s) and $\dot{m}_a$ is the mass flow rate of air (kg/s) and the subscript "stoich" refers to these values under stoichiometric conditions. Note that to calculate ϕ, also the quotient of the actual fuel/oxygen ratio and the stoichiometric fuel/oxygen ratio could be used.

As discussed in Chap. 2, there are different terms used for different ventilation conditions. The situation when more air (oxygen) is available than is needed for stoichiometric combustion, is referred to as overventilated, well-ventilated, fuel lean, or fuel controlled. If insufficient air is available for stoichiometric combustion the situation is termed under ventilated, vitiated, fuel rich, or ventilation controlled. Note that in some publications the words do not mean exactly the same thing. In this chapter, the terms well-ventilated (fuel controlled) and under ventilated (ventilation controlled), respectively, are mainly used and are related to the whole system. Even under well-ventilated conditions, the geometric conditions and flow pattern can be such that fresh air does not reach the combustion zone. Such a situation is here referred to as locally under ventilated. In Sect. 7.5, the effect of the ventilation conditions on the production of different species are further discussed.

---

[2] see also Eq. (2.14).

To be able to relate the produced amount of a certain species to the consumed mass of fuel, it is of interest to know the net heat of combustion, ΔH_c (kJ/kg), which is defined as the enthalpy change for a complete reaction where 1 kg fuel reacts with O_2 to yield CO_2 and H_2O at a given temperature and pressure (298 K and 1 atm, respectively), that is, the difference between the total enthalpy of formation of the products and the total enthalpy of formation of the reactants. By default, the heat of combustion used here corresponds to product of water in vapour form (often referred to as net heat of combustion). To find ΔH_c the following expression is used:

$$\Delta H_c = \sum_{products} \Delta H_f - \sum_{reactants} \Delta H_f \tag{7.9}$$

where ΔH_c is the enthalpy of formation (kJ/kg).

If energy is released from the reaction, ΔH_c will be negative, but note that in many tables for different fuels, heat of combustion is given as a positive value. If now the heat of combustion is known (or assumed to be an average value) and the heat release is measured, the mass loss of fuel, $\dot{m}_f$, can be calculated as

$$\dot{m}_f = \frac{\dot{Q}}{\chi \cdot \Delta H_c} \tag{7.10}$$

where $\dot{Q}$ is the heat release rate (HRR) (kW) and χ is the combustion efficiency. Through substitution of Eq. (7.10) into Eq. (7.8), one obtains:

$$\phi = \frac{\dot{Q} \cdot r}{\dot{m}_a \cdot \Delta H_c \cdot \chi} \tag{7.11}$$

Hugget showed that $\Delta H_c/r$ is approximately 3000 kJ/kg, consumed air for most carbon-based materials [14]. This leads to the equation[3]

$$\phi = \frac{\dot{Q}}{\dot{m}_a \cdot 3000 \cdot \chi} \tag{7.12}$$

if the HRR is given in kW.

7.3 Yields

To compare the emissions from different materials, yields, Y_i (kg/kg), are introduced and widely used (in most of the tables in this chapter they are given as g/kg). This means the ratio between the mass m_i (kg) of a compound i generated by the combustion of a certain mass of material (fuel):

---

[3] See also Eq. (2.17).

Table 7.2 Yields of CO (g/kg) for different experimental set-up and varied combustion conditions

Material	Large-scale tests[a] [16]	Small-scale method[b] [17]
Wood	58	5[c]
Paper	58	
Textiles	51	
PVC	116	63
PUR	160	20–50[d]
Polystyrene	220	60
Polyethene	60	24

[a] Values taken from a summary of yields during large-scale fire tests. Ventilation conditions might have been different between the different tests performed in large-scale and small-scale

[b] ASTM E2058 fire propagation apparatus

[c] Pine

[d] Rigid PUR

$$Y_i = \frac{\dot{m}_i}{\dot{m}_f} \quad \text{or} \quad Y_i = \frac{m_i}{\Delta m_f} \tag{7.13}$$

where $\dot{m}_i$ is the production rate of compound i (kg/s) and $\dot{m}_f$ is the mass loss rate of fuel (kg/s), Δm_f is the total fuel mass loss (kg) during the studied test period. Equation (7.13) shows that one can use either mass flow rates, $\dot{m}_i$, or total mass, m_i, of the produced species to calculate the yield. However, one must realize that the latter method gives some overall average results and that different materials might be consumed at different times during the fire (or experiment). Therefore, the results obtained might be more useful if these differences could be resolved. In this section, examples of yields of different products from some common materials are presented. Much of the yields below were summarized by Lönnermark et al. [15].

Yields of CO from some common materials used in fire experiments in different scales are presented in Table 7.2. The yields in the table, as well as most of the other tables in this chapter are given with the unit g/kg. Note that the yields in large-scale tests generally are higher than the yields in the small-scale tests. These differences could be due to scaling effects, geometrical differences or differences in ventilation and combustion conditions. It should, however, be noted that the large-scale values in Table 7.2, are based not only on experimental values but also on considerations of chemical composition and experimental conditions.

Hertzberg et al. tested in the cone calorimeter (ISO 5660-1 [18]) a large number of different materials [19]. The yield of particles can be found in Table 7.3.

Butler and Mulholland [20] made a summary of smoke yields (can probably be described as soot yield, but the wording of the authors has been used here) from different plastic materials. A selection of their data is presented in Table 7.4. Yields of

Table 7.3 Yield of particles from materials tested in the cone calorimeter [19]

Material	Particle yield (g/kg)
FR4, brominated laminate	139
Polystyrene (EPS)	126
Teflon-cable	102
Carbon fibre laminate	83
PVC (floor)	57
Polyethene-cable	51
50 % PVC + 50 % Teflon cables	42
PVC-cable	39
Bitumen	38
Polyethene pellets	35
Stone wool	30
Optic cable	29
Glass wool	28
Polyurethane (PUR), rigid	26
Teflon pellets	25
Nitrile rubber	25
Wool (92 % wool, 8 % polyamide)	22
Melamine	18
Particle board	3.9
Wood	2.4

Table 7.4 Yield of smoke from different plastic materials [20]

Material	Fuel surface (m^2)	Smoke yield (g/kg)
PMMA	0.006	15–18
Polystyrene	0.006	41
PVC	0.006	105–185
Rigid PVC	0.006	12
Polypropene	0.006	42
Rigid PUR	0.006	91
Flexible PUR	0.0225	34
HDPE	0.006	18–23

CO, CO_2, total hydrocarbons, and smoke from different plastic materials, based on small-scale experiments, are summarized in Table 7.5.

Tewarson [17] presents yields for CO, total hydrocarbons and smoke for a large number of materials based on small-scale tests. The yields for some liquid fuels are given in Table 7.6.

Table 7.5 Yield of CO, CO_2, total amount of hydrocarbons (THC) and smoke for some common plastic materials (g/kg) [17]

Material	CO	CO_2	THC	Smoke
ABS				105
PMMA	10	2120	1	22
Polyethene	24	2760	7	60
Polypropene	24	2790	6	59
Polystyrene	60	2330	14	164
Nylon	38	2060	16	75
PVC	63	460	23	172
EPS	54	1900		

Table 7.6 Yield of CO, hydrocarbons and smoke from some common liquid fuels (g/kg). The values come from small-scale tests [17]

Material	CO	Hydrocarbons (HC)	Smoke
Methanol	1	–	–
Ethanol	1	1	8
Isopropyl alcohol	3	1	15
Acetone	3	1	14
Heptane	10	4	37
Kerosene	12	4	42
Benzene	67	18	181
Mineral oil	41	12	97

7.4 Emissions from Fires in Vehicles and Tunnels

There are a number of reports and papers on the issue of fires and the environment. Some of them present summaries of emissions from common materials or common types of fires [16, 21, 22], while others focus on emissions from fires in a more general sense or present results from single fires that have had a large impact on the environment [23–25].

The analysis of the smoke gases from an automobile fire (passenger car) shows that emissions with a potentially negative impact on the environment, or humans, are produced in significant concentrations [26]. Three separate, full scale fire tests were performed under SP's large-scale ("industry") calorimeter: a fire ignited and developed in the engine compartment; a fire ignited inside the vehicle that was extinguished in the early stages; and a similar fire ignited inside the vehicle that was allowed to spread until the entire vehicle was involved in the fire. Both fire gases and run-off water were analysed.

The emissions included HCl, SO_2, volatile organic compounds (VOCs; for example, benzene), polycyclic aromatic hydrocarbons (PAHs), and polychlorinated

Table 7.7 Emissions of PCDD/F and PAH from vehicle fires in a tunnel and PCDD/F found in the fire residue [28]. The values are divided by the energy content

Vehicle	Q_{tot}	Fire residue PCDD/F		Tunnel PCDD/F		Tunnel PAH	
	GJ	mg I-TEQ	mg I-TEQ/GJ	mg I-TEQ	mg I-TEQ/GJ	g	g/GJ
Old car	6	0.012	0.002	0.032	0.0053	13	2.2
New car	9	0.008	0.00089	0.044	0.0049	27	3.0
Subway carriage	41	0.54	0.013	2.0	0.049	NA	NA
ICE-wagon	77	1.1	0.014	9.2	0.12	NA	NA

dibenzo-p-dioxins and dibenzofurans (PCDDs/PCDFs). The definition of VOC often depends on the sampling/analysis method, but typically include species with molecular masses between 75 and 200 g/mol. Sources of chlorine in the vehicle for production of HCl and PCDDs/PCDFs included, most probably: upholstering materials, dash board components, and electrical wirings, as indicated from the small-scale experiments conducted on selected materials from an automobile similar to that used for the full scale automobile fire.

Aldehydes and isocyanates were also found in the smoke gases, both compounds with well-documented short-term and long-term effects on humans. Other toxic compounds included: HCN and SO_2. These compounds have a direct effect on people and are of concern for rescue personal and others exposed to smoke from vehicle fires. The health effects, especially time to incapacitating dose for some of the gases, are further discussed in Chap. 15.

The particles emitted from the fire had a particle size distribution with a high number of particles with a diameter below 1 μm. Such small particles can be transported far from the location of the fire and are respirable, implying that the body's defence system against particles (in the nose and throat) cannot provide adequate protection. Analysis of the content of the fire-generated particles revealed that these contained high concentrations of zinc, lead, and chlorine.

Analysis of extinguishing water showed that this was severely contaminated, containing elevated levels of both organic compounds and metals. Comparison with data from other vehicle fires found in the literature showed that contamination of lead, copper, zinc, and antimony appear to be significant in water run-off from these types of fires.

Within the EUREKA EU499 project [27] the release of PCDD/Fs and PAHs were analysed in connection with some of the tests: an old car (1974), a new car (1988), a German subway carriage, and a Deutsche Bahn wagon with a steel body and a modern InterCityExpress (ICE) interior [28], see further Chap. 3, Sect. 3.3.7. The release into the tunnel was estimated by using 1 m^2 passive collectors (cotton and steel, respectively) and active sampling at different positions along the tunnel. In addition, the fire residue was analysed. In Table 7.7 the releases of PCDD/F and PAH into the tunnel from the different vehicle fires are summarized. To better compare the results with results from other tests, the values have been normalized relative to the energy content of each vehicle. The results show that the PCDD/F from the subway carriage and the ICE-wagon are similar and that these results are approximately one order of magnitude larger than those from the passenger cars. Corresponding values obtained in the passenger car fires described above [26] were 0.023 mg I-TEQ/GJ (0.0868 mg I-TEQ in total) for PCDD/F and 31.3 g/GJ (119 g in total) for PAH, that is, almost an order of magnitude higher than for the cars reported by Wichmann. Apart from actual differences in production between the tests, there are two other possible explanations for the differences. There might be higher collection efficiency in the tests performed beneath the industry calorimeter. There is also a difference in how the total energy was calculated. In the case of the EUREKA 499 tests, the energy content was estimated from the composition of the fuel load, while in the test presented by Lönnermark and Blomqvist [26] the total energy was calculated from the heat release measurements. This latter difference is, however, relatively small. A comparison with the integrated values available for the subway carriage and the ICE-wagon [29], show that the estimated total energy content is approximately 10 % higher than the integrated HRR value for the subway carriage and approximately 30 % higher for the ICE-wagon.

Lönnermark and Blomqvist [26] present yield result from fire tests with a car and materials from a car. The emissions of the main combustion products from selected materials are listed in Table 7.8. The materials were selected to represent the most abundant combustible materials in the car. There was no information available on the amount of respective material in the car. However, in the work done by Persson et al. [22] one assessed that, for example, 9 % of the plastic material of an automobile was PVC and 17 % was PUR.

The test set-up used for the small-scale fire tests was the closed 0.5 m^3 chamber described in ISO 5659. The 75 × 75 mm horizontally mounted sample was exposed to two different levels of external radiation in consecutive tests. A lower radiation level of 25 kW/m^2 was applied to generate pyrolytic conditions, and a higher level of 50 kW/m^2 was applied to give conditions of flaming combustion.

The yields of the inorganic gas components from the full scale tests with a car are presented in Table 7.9.

Much referred to is the work by Lemieux et al. [30–33]. During tests with pieces of car tyres, measurements were made of VOC, semi-VOC, particles, PAH, and some metals. In the tests either "chunk", (1/4–1/6 tires) or "shred" (5.1 × 5.1 cm) tires were combusted in a "burn pit" [32]. In total 13.6 kg (approximately two tires) were placed on a scale. Between 4.5 and 9.0 kg was combusted. In Table 7.10, selected results from the VOC analyses are presented.

Conesa et al. [34] performed pyrolysis experiments in laboratory scale with pieces of car tyres. The pieces had a diameter of approximately 4 mm. The flow of fuel was 0.5 g/min. By controlling and varying a flow with a mixture of O_2 and N_2, yields under different conditions (pure N_2 or 10 % O_2) could be calculated. Also the temperature was varied: 450, 750, and 1000 °C. The main species found were CO_2, CO, H_2, methane, ethane, propane, propene, isoprene, benzene, and toluene. The results are presented in Table 7.11. There is a clear function of the temperature,

Table 7.8 Yields of compounds generated by the combustion of materials found in cars. Results from small-scale tests [26]

Car component	Test condition	CO_2 (g/kg)	CO (g/kg)	HCN (g/kg)	NO (g/kg)	NH_3 (g/kg)	HCl (g/kg)	SO_2 (g/kg)
Door panel	Pyrolytic	410	43	2.1	–	–	120	–
	Flaming	1500	72	2.9	7.4	-	160	–
Component from ventilation system (polymer)	Pyrolytic	–	360	–	–	–	–	–
	Flaming	2100	27	–	–	–	–	–
Floor material (carpet)	Pyrolytic	–	49	4.9	–	–	–	–
	Flaming	2400	43	0.9	9.5	–	–	–
Dashboard	Pyrolytic	260	25	3.8	–	–	–	–
	Flaming	1800	23	1.2	6.4	–	–	–
Upholster material from driver's seat	Pyrolytic	250	43	1.7	–	–	51	–
	Flaming	1800	78	2.4	5.7	0.4	66	9.9
Upholster material from back seat	Pyrolytic	–	26	3.9	–	–	–	–
	Flaming	1700	88	5.3	7.5	0.35	8.1	10
Lacquered plate from car body	Pyrolytic	–	21	–	–	–	–	–
	Flaming	610	96	2.7	–	–	–	–
Electrical wirings	Pyrolytic	260	32	–	–	–	340	–
	Flaming	1100	86	–	–	–	390	–
Tyre	Pyrolytic	–	81	–	–	–	–	21
	Flaming	1400	30	–	–	2.3	–	11

Table 7.9 Yield for inorganic gas components during full scale tests with a car [26]

Species	Total amount (kg)	Yield (g/kg)
CO_2	265	2400
CO	6.9	63
HCN	0.17	1.6
HCl	1.4	13
SO_2	0.54	5.0

Table 7.10 Yields of selected VOC species from pieces of car tyres during small-scale tests, sampled with two different methods: VOST (Tenax-GC) and XAD-2, respectively [32]

Species	Yield (Chunk) (g/kg)	Yield (Shred) (g/kg)
VOST (Tenax-GC)		
Benzene	2.16	2.20
Phenol	0.0005	0.014
Total	11.2	13.1
XAD-2		
Biphenyl	0.21	0.33
Phenol	0.37	0.70
Total	8.37	16.3

Table 7.11 Yields of selected species in gas phase from pyrolysis tests in laboratory scale with pieces of car tyres (g/kg) [34]. Two different atmospheres were used: 100 % N_2 and a mixture of 90 % N_2 and 10 % O_2. Values are average of two tests if not else stated

Species	450 °C		750 °C		1000 °C	
	0 % O_2	10 % O_2	0 % O_2	10 % O_2	0 % O_2	10 % O_2
CO_2	34	85	41	100	18	45
CO	–	47	12[a]	36	13	89
H_2	0.5	2.9	3.5	4.0	10	13.8
Methane	6.5	11	46	48	79	38
Ethane	2.4	1.3	11	11	1.1	0.4
Ethene	3.9	1.7	24	28	7.1	3.1
Propane	0.9	0.8	1.4	1.4	0.02[a]	–
Propene	2.2	1.0	11	16	0.34	0.06
Isoprene	29	3.6	7.2	3.0	0.15[a]	–
Benzene	–	–	43	45	87	77
Toluene	0.03	15	25	21	–	0.03

[a] Detected only in one test

especially for the last three species. They were, however, analyzed only in the gas phase and the total emissions could have been higher.

Vianello et al. [35] developed a scale-model car (scale 1:30) to perform fire tests in a scale tunnel (total length 5.0 m, radius 0.15 m, height from the floor to the apex 0.21 m, and width 0.30 m). The tunnel was naturally ventilated. The main purpose of the test series was to study the temperature profiles in the tunnel and compare with real scale. During the tests, however, samples for gas analyses were also extracted. Four different types of adsorber/filter were used: Tenax, XAD-2, Silica gel, and PTFE/glass fibre. The results are presented in Table 7.12.

Lemieux et al. [33] presented average values to represent yields from cars, boats, and trains for the following species: CO (62.4 g/kg), particles (50.0 g/kg) and NO (2.0 g/kg).

In the Runehamar tunnel large-scale tests, mixtures of cellulose and plastic materials were used as fuels [36–38]. The test data clearly show that the production rate of CO_2 increases linearly with the HRR (see Fig. 7.1). The relation can be expressed as [36]:

$$\dot{m}_{CO_2} = 0.087\dot{Q} \tag{7.14}$$

where the HRR is given in MW.

Note that different materials were used in the Runehamar tunnel fire tests, including wood pallets, PE materials, PUR mattresses, furniture, and paper cartons with polystyrene cups. It seems that for these types of materials the production rates of CO_2 are independent of the materials and only dependent on the HRR. The

Table 7.12 Results from sampling during fire in a scale-model car in a scale tunnel [35]

Compound	Concentration
Tenax adsorber	[mg/m^3]
Benzene	0.415
Toluene	0.380
Ethyl benzene	0.015
p-zilene	0.056
m-xilene	0.053
o-xilene	0.027
XAD-2 adsorber	[mg/m^3]
Naphtalene	0.607
Acenaphtylene	0.136
Silica gel adsorber	[µg/m^3]
HF	0.087
HCl	0.165
HNO_3	0.707
H_2SO_4	0.790
PTFE filter and glass fibre	[mg/m^3]
Anthracene	0.576
Fenanthrene	0.587
Fluoranthene	0.536
Pyrene	0.437
Benzo[a]anthracene	0.172
Crisene	0.191
Benzo[a]pyrene	0.128
Benzo[b]fluoranthene	0.169
Benzo[k]fluoranthene	0.136
Indeno[1, 2, 3-cd]pyrene	0.114
Benzo[g, h, i]perylene	0.095

reason could probably be that the main fire load consisted of the cellulose materials and that the combustion efficiency was high during large portions of the tests.

However, there was no simple correlation between the production rate of CO and the HRR (see Fig. 7.2). The production rate of CO strongly depends on the type and geometry of the fuels, which influence the access of air and local ventilation and burning conditions. Most of the CO was produced at the beginning of each test in the Runehamar tunnel fire tests when the combustion seems to have been less efficient and in the rest of each test the combustion appears to have been very good, with the possible exception of the test T2, which involved PUR. The short period of less efficient combustion was, however, enough to have significant influence on the CO results.

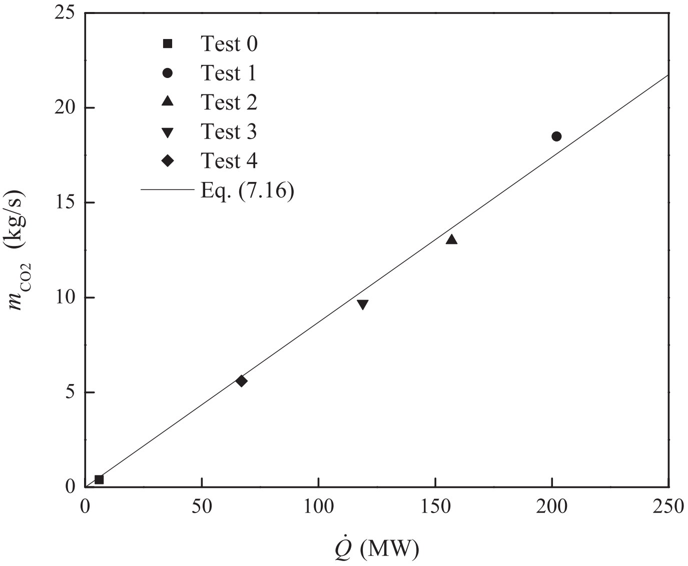

Fig. 7.1 The production rate of CO_2 as a function of the HRR from large-scale tests in the Runehamar tunnel [36]

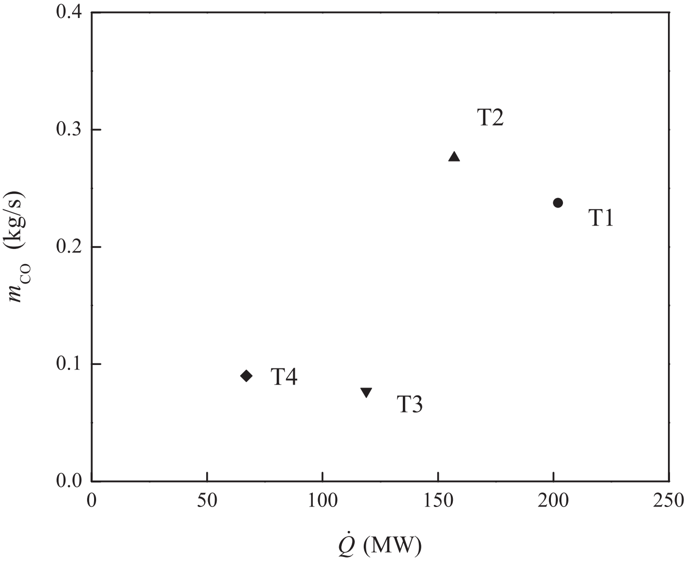

Fig. 7.2 The production rate of CO as a function of the HRR from large-scale tests in the Runehamar tunnel [36]

7.5 Effect of Ventilation Condition

The ventilation conditions are important for the chemical production and the hazards (see Chap. 15). In an under ventilated fire situation the yield of major toxicants (for example, carbon monoxide and hydrogen cyanide) is greater, compared to well-ventilated conditions. Furthermore, the total volume of effluents is greater [39].

The ventilation is an important means to affect, and hopefully improve, the conditions in a tunnel. Longitudinal ventilation can improve the conditions upstream of the fire significantly, making it possible for the rescue service to reach the fire. It is, however, important to remember that the situation downstream of the fire can be exacerbated by the ventilation. In Norway, at least at some places, the ventilation is used as a part of the firefighting tactics where in case of fire the ventilation is used in a predefined direction [40]. Two reasons in particular are given for this methodology: first, the firefighters know in advance the ventilation direction in the tunnel and thereby what portal to attack the fire from, and second, the conditions downstream of the fire are assumed to be of no danger to people being in this part of the tunnel, due to dilution of the fire gases. This strategy is partly based on the results from the experiments with two passenger cars in the Byfjord tunnel in 1998 and the Bømlafjord tunnel in 2000. These results showed that downstream of the car fires, the concentrations of CO and NO_x were not life threatening [41].

In a Swedish study concerning the HRRs from tunnel fires, the ability of the rescue service to rescue people from the tunnel and to attack the fire, and the possibility for people to escape from a tunnel fire showed that the two main effects of longitudinal ventilation on the conditions during a tunnel fire is an increase of the growth rate of the fire and an increased dilution of the gases [42].

The ventilation conditions can be described by the equivalence ratio as defined in Sect. 7.2 and Eq. (7.8). The local ventilation conditions can be very important for the combustion process, but in cases where the spatial variation either can be assumed to be small or when it is difficult to resolve the variations, the overall combustion process is often studied instead. In such cases ϕ can be defined in a more general sense using the equivalence ratio for the total combustion process. This is usually referred to as the global equivalence ratio (GER). Originally, the GER was defined as the ratio of the mass of gas in the upper layer in an enclosure derived from the fuel divided by that introduced from air, normalized by the stoichiometric ratio [43]. Beyler, who was the first to correlate the species concentrations in the upper layer with the equivalence ratio, used a variant called the plume equivalence ratio defined as the ratio of the fuel volatilization rate to the air entrainment rate, normalized by the stoichiometric fuel to air ratio [44–46]. In the work presented by Blomqvist and Lönnermark [47], the definition of the GER is the ratio between the mass loss rate of the fuel and the mass flow of oxygen entering the combustion room normalized by the stoichiometric ratio.

In order to measure the GER in the two different test rooms used by Blomqvist and Lönnermark, a device called "the phi meter" [48, 49], was constructed. The essential parts of the phi meter are the combustor, into which the fire gases and additional pure oxygen are introduced, and the O_2 analyser. Complete combustion of the fire gases is achieved in the combustor by the high temperature (1000 °C was used in these specific tests) and by using a platinum catalyst and additional oxygen. The readings on the O_2 analyser are compared with background measurements without fire gases through the phi meter. A simple computation gives the equivalence ratio [47].

There are not many cases reported on measured under ventilated conditions in fires in tunnels. Most cases reported can probably be said to be either fuel controlled or ventilation controlled (for example, see [50]). The latter correspond to a case where limited ventilation leads to a decrease (or control) in the fire size, but if the temperature is high, a continuous mass loss can lead to under ventilated combustion. Among the large-scale fire test series, the one in the Ofenegg tunnel is an obvious example of the effect of the ventilation (see Chap. 3), but that case was also rather special due to the blockage at one end of the tunnel.

Ingason [51, 52] performed fire tests in a model tunnel ($1.08 \times 1.2 \times 10.96$ m^3) to study the effect of the ventilation on the fire behaviour. Under ventilated conditions were of special interest and both naturally ventilated and forced ventilated scenarios were studied. In the first series of tests with naturally ventilated scenarios the fire size and the size of the inlet opening were varied, while in the second series of tests with forced ventilated scenarios the fire size and the flow rate of incoming air were varied. The author described the difficulty in achieving under ventilated condition. The transition to such conditions is highly dependent on the temperature and the thermal feedback to the fuel. This was also seen in the test series described by Lönnermark et al. [53], where a case with 0.5 m^2 chlorobenzene (test CB3) gave a very slow developing fire inside a room. The fire reached high temperatures and under ventilated conditions first after approximately 35 min. Increasing the pool size to 0.8 m^2 (test CB4) gave a significantly different fire development with much higher temperatures and under ventilated conditions after approximately 6 min. This illustrates the importance of the fire size. In a tunnel with forced ventilation, the flame tilt also influences the thermal feedback and thereby the fuel mass loss rate.

In the test series presented by Ingason [51, 52] some of the tests, however, became under ventilated. Gas compositions (CO, CO_2, and O_2) were analysed at three different heights (0.15, 0.5, and 0.9 m below the ceiling), 4.5 m downstream of the centre of the fire, which was situated 1.5 m from the tunnel entrance. The results were presented as $\Delta CO/\Delta CO_2$ ratios, which is the ratio between the increase in CO volume concentration and increase in CO_2 volume concentration. Note that in some of the work referred below instead the ratio between the actual CO volume concentration and the actual CO_2 volume concentration (CO/CO_2 ratio) was used. The version used in the original publication has also been used in this chapter.

In most of the tests presented by Ingason, the $\Delta CO/\Delta CO_2$ ratios were rather similar at the different sampling heights. The ratio was, however, often somewhat higher in the highest position (0.15 m below the ceiling) during some period of the tests. In a few cases the $\Delta CO/\Delta CO_2$ ratio was highest in the lowest position (for example, in test 2 and test 8). In Fig. 7.3 the $\Delta CO/\Delta CO_2$ ratios for heptane pool fires are presented as a function of the equivalence ratio. The values were chosen

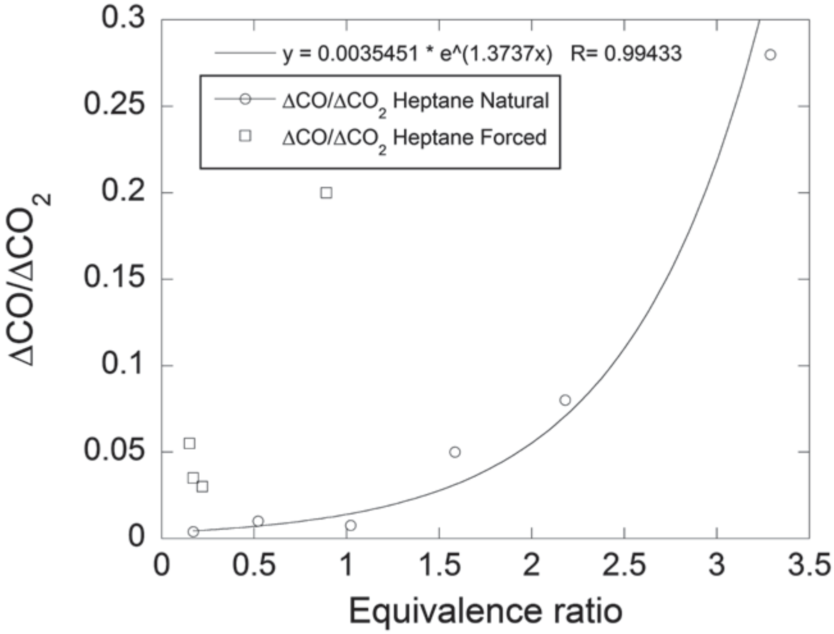

Fig. 7.3 $\Delta CO/\Delta CO_2$ ratio as function of equivalence ratio for heptane pool fires performed by Ingason [51, 52]. The results are given both for natural ventilation and for forced ventilation. Included for illustration is an exponential curve fit of the natural ventilation data [54]. It is, however, based on only six data points

to be representative values for the position with the highest $\Delta CO/\Delta CO_2$ ratio at the selected time. Note that Ingason used an equivalence ratio based on the air to fuel ratio, while throughout this book all equivalence ratios (including those presented in Fig. 7.3) are based on fuel to air ratios. Two different cases are represented in the figure: natural ventilation and forced ventilation. The values of the $\Delta CO/\Delta CO_2$ ratios were determined at the time when the mass loss rate was at its maximum for each test. For the natural ventilation an exponential curve fit is included [54]. It fits the data points very well, but due to the limited number of points it should only be seen as an illustration.

The points for the forced ventilation show a pattern very different from that in the natural ventilation cases. All cases are well-ventilated, but the point at $\phi = 0.89$ shows features of under ventilated fires. This could have two possible explanations. There are studies that indicate that the CO production starts to increase well below $\phi = 1$, at $\phi \approx 0.6$ (see for example, [44, 43]).

Another explanation could be the flow pattern around the fire during forced ventilation. The experimental results, especially the O_2 measurements, show a significant gradient with height, which indicates that even if the tunnel is well-ventilated it could be locally under ventilated in the combustion zone. The three-dimensional flow typically found close to the fire in a tunnel was illustrated by Ingason, showing the main ways for the flows of different density [55].

Table 7.13 $\Delta CO/\Delta CO_2$ ratio as function of equivalence ratio for xylene and methanol pool fires performed by Ingason [51, 52]

Fuel	Ventilation	Fire size [m^2]	Opening [m^2]	ϕ	$\Delta CO/\Delta CO_2$
Xylene	Natural	0.3 × 0.3	0.3 × 0.3	0.37	0.20 (0.38)[a]
Xylene	Natural	0.3 × 0.3	0.15 × 0.15	1.01	0.30 (0.41)[a]
Xylene	Natural	0.3 × 0.3	0.1 × 0.1	1.94	0.36 (0.43)[a]
Xylene	Natural	0.3 × 0.3	0.2 × 0.2	0.70	0.23 (0.31)[a]
Xylene	Forced	0.3 × 0.3	0.2 (ø = 0.5 m)	0.15	0.15 (0.26)[a]
Methanol	Natural	0.4 × 0.4	0.6 × 0.6	0.04	0.003–0.035[b]
Methanol	Forced	0.4 × 0.4	0.2 (ø = 0.5 m)	0.02	−0.01–0.02[b]

[a] The $\Delta CO/\Delta CO_2$ ratio was highest in the beginning of the result period reported and then decreased; the maximum value (within parenthesis) is not used (see discussion of Fig. 7.2) but instead something closer to a steady state value

[b] The $\Delta CO/\Delta CO_2$ ratio is varying significantly; therefore a range is given (including all the three heights)

Results from the experiments with xylene and methanol are summarized in Table 7.13. Compared to the experiments with heptane pool fires presented in Fig. 7.3, xylene results in high values and methanol in low values of $\Delta CO/\Delta CO_2$ ratios. This is in line with the results of Beyler [44] showing that oxygenated hydrocarbons produce small amounts of CO (expressed as yield) at low equivalence ratios. Aromatics (Beyler used toluene) on the other hand, produce a rather constant CO yield independent of the equivalence ratio; only a small increase was reported. This means that aromatics at low equivalence ratios produce relatively high CO yields and at high equivalence ratios produce relatively low CO yields. The variation in $\Delta CO/\Delta CO_2$ ratio with equivalence ratio presented in Table 7.13 might be explained by a decrease in CO_2 production.

Lönnermark et al. [53] performed under ventilated fire experiments in an enclosure (the ISO 5705 room: 2.4×3.6×2.4 m^3), where the size of the opening was varied. Five different fuels were used: Polypropene, Nylon 66, Tetramethylthiuram monosulfide, 3-Chloro-4 nitro-benzoic acid, and Chlorobenzene. In the paper by Blomqvist and Lönnermark [47] results are given for CO and other components in the fire gases, and their dependence on the equivalence ratio. For comparison with the results from model scale tunnel tests presented in Fig. 7.3, CO/CO_2 ratios have been calculated from tests in the enclosure fires [53]. Note that here absolute concentrations have been used, and not changes from background values as in the case presented by Ingason.

In Fig. 7.4, CO/CO_2 ratios for polypropene, Nylon 66, and chlorobenzene pool fires (polypropene and Nylon 66 were solid polymers in form of pellets) are presented as function of the equivalence ratio. For all three materials, results are presented for measurements both in the opening from the enclosure and in the exhaust duct connected to the hood collecting the fire gases. For illustration, an exponential

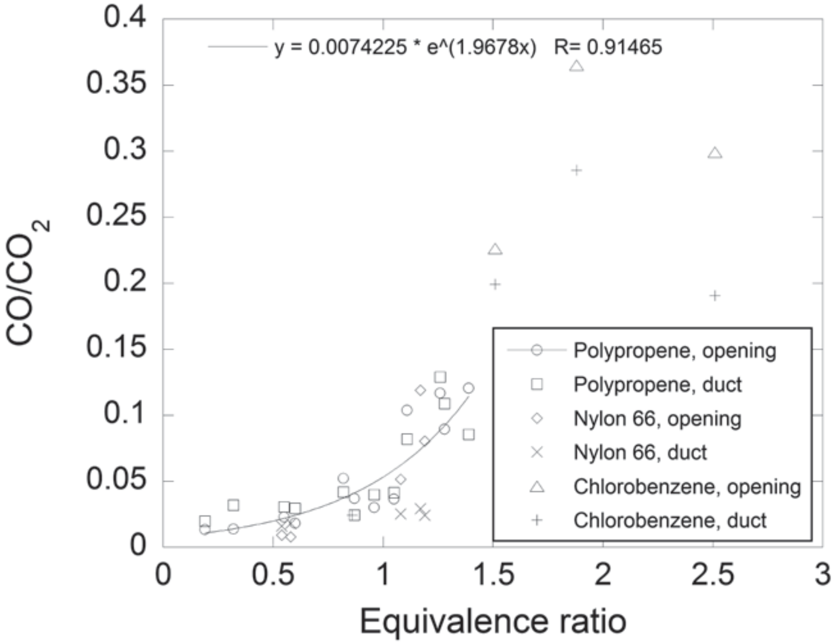

Fig. 7.4 CO/CO_2 ratio as function of equivalence ratio for polypropene, Nylon 66, and chlorobenzene. For all three materials, results are given for measurements in the opening of the enclosure and in the exhaust duct connected to the hood collecting the fire gases. An exponential curve fit is included for polypropene (opening) [54]

curve-fit for the results from the opening for polypropene is included. This fit seems to be qualitatively representative for the other cases also, even if there are differences between the materials.

The effect of combustion outside the opening during under ventilated conditions can be seen for Nylon 66. This effect is also obvious for chlorobenzene. For heptane the CO/CO_2 ratio are rather similar in the opening and the duct for most values of the equivalence ratios reported. From the figure it can be seen that when passing from well-ventilated to under ventilated conditions (passing the point $\phi = 1$), the CO/CO_2 ratios increases above approximately 0.05. This is comparable to the natural ventilated tests with heptane in the model scale tunnel performed by Ingason (see Fig. 7.3). For the cases with forced ventilation the differences are larger. The explanations for this, besides differences between materials, were discussed earlier.

Grant and Drysdale [56] presented analyses of CO and CO_2 for the EUREKA EU499 project. The calculated CO/CO_2 ratios show that high values (maximum 0.2, 30 m downstream of the fire and 0.13, 100 m downstream of the fire) are obtained during the initial phase before the HRR starts to increase rapidly, that is, when the fire spreads to the trailer. During the most intense part of the fire, the CO/CO_2 ratios 100 m downstream stay below 0.02. At 30 m downstream of the fire the CO/CO_2 ratio are also approximately 0.02 or lower, but a clear increase during

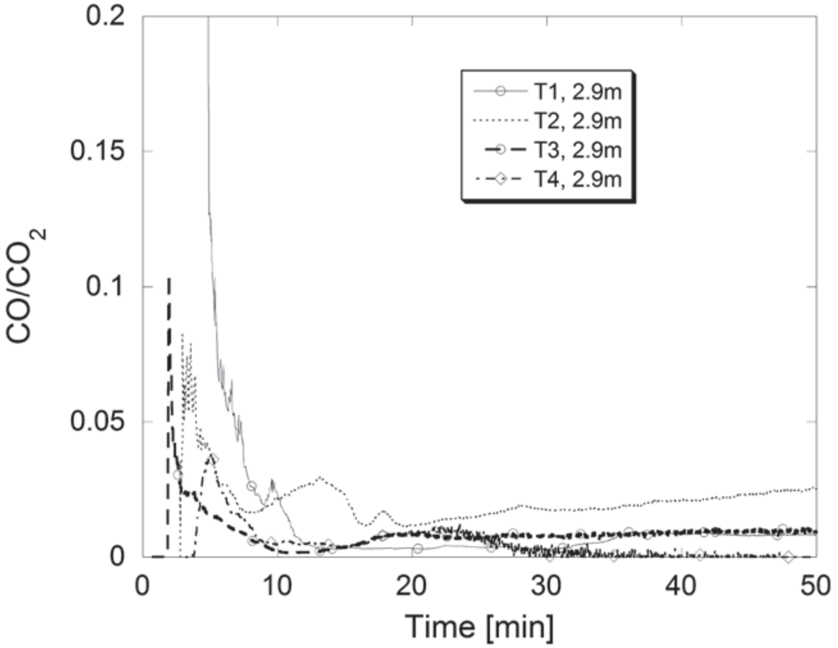

Fig. 7.5 CO/CO$_2$ ratio as function of time for the Runehamar tests. The gas analyses were performed at 458 m from the centre of the fire, 2.9 m above the road surface [54]

the period when the ventilation was switched off can be seen. The maximum value given is 0.05, but the peak value during this time period could be higher since values are missing for a few minutes. Comparing these results with those presented in Figs. 7.3 and 7.4 indicates under-ventilated combustion during this time period, which is understandable due to low ventilation during a period of high temperatures and probably high mass loss rates.

Similar results were found in the four Runehamar tests, that is, high CO/CO$_2$ ratios during the initial phase of the fire and low values during the intense fire and the decay period (see Fig. 7.5). The gas analyses (CO and CO$_2$) were performed at two different heights (2.9 and 5.1 m respectively above the road surface), 458 m from the centre of the fire. Analyses of O$_2$ were also performed in these positions and at the height 0.7 m (see the work by Ingason et al. [36, 37] for detailed description of the measurement setup and analysers). It can be seen from Fig. 7.5 (in comparison to Fig. 7.4) that all the tests are well-ventilated [54]. The high values at the beginning of the tests can be explained by incomplete combustion. The temperature in the combustion zone may have affected the results. It is known from fire experiments in compartments that both the residence time and the temperature in the upper layer are important factors for the production of CO [57]. Even for well-ventilated conditions, high CO concentrations can be measured if the temperature is below approximately 800 K. The situation looks similar to the one called preflaming combustion described by Tsuchiya and discussed below [58]. The highest values (not shown in the figure) are also dependent on the absolute relationship between the CO and CO_2 analyses. A small difference in response time or time to reach a concentration above the detection limit, significantly affects the initial values. To be able to compare the CO/CO_2 ratios better with the HRR and the temperature measurements near the fire, the time scales in Fig. 7.5 were corrected for the transport time between the fire and the measurement station. This transport time varies with the HRR and the procedure to calculate this is described by Ingason and Lönnermark [37]. The estimated transport time varies between 1.5 and 2.5 min depending on the HRR.

The results from the Runehamar tests look similar to those reported by Bettis et al. [59] where the tests were well-ventilated, apart from a short period during one of the tests. The CO/CO_2 ratios ranged, in most cases, from 0.005 to 0.025. In a few cases there was a higher value (0.05–>0.1) in the beginning of the test followed by a continuous decrease. A steady state value as high as 0.05–0.06 was reported in only one test (Test 6). The fire was partly sheltered due to the setup and this may have affected the local ventilation conditions.

During ventilated conditions in a tunnel, the situation at the fuel can be ventilation controlled or locally under ventilated if the fuel setup is such that the air flow does not reach the vaporized or pyrolized fuel. This was mentioned in relation to the initial period of fires discussed above.

Tewarson [17] performed an extensive work on collecting data on yield of CO and CO_2, respectively, for different materials, and on how these yields depend on the equivalence ratio. From the result he developed relationships of the ratio of actual yield to well-ventilated yield as function of equivalence ratio. For CO Tewarson suggested the following relation:

$$\frac{Y_{CO,uv}}{Y_{CO,vv}} = 1 + \frac{\alpha}{e^{2.5\phi^{-\xi}}} \tag{7.15}$$

where the values of correlation parameters for some selected fuels are presented in Table 7.14. Combining his results for CO and CO_2 gives the following equation [54]:

$$\frac{X_{\mathrm{CO}}}{X_{\mathrm{CO_2}}} = \frac{44\left[1 + \dfrac{\beta}{\exp\left(2.5\phi^{-\xi}\right)}\right] Y_{CO,wv}}{28\left[1 - \dfrac{1}{\exp\left(\left(\phi/2.15\right)^{-1.2}\right)}\right] Y_{CO_2,wv}} \tag{7.16}$$

where Y is the yield [kg/kg], β and ξ are correlation coefficients, X is the volume concentration and the index wv corresponds to well-ventilated conditions. The values of the different parameters are given for four selected materials in Table 7.14. The CO/CO_2 ratio as a function of ϕ based on Eq. (7.16) is given for three materials

Table 7.14 Yields of CO and CO_2 during well-ventilated conditions and values of correlation coefficients in Eq. (7.16) given for four materials [17]

Material	$y_{CO,wv}$ [kg/kg]	$y_{CO_2,wv}$ [kg/kg]	α	β	ξ
Polyethene (PE)	0.024	2.76	10	10	2.8
Polypropene (PP)	0.024	2.79	10	10	2.8
Polystyrene (PS)	0.060	2.33	2	2	2.5
Wood	0.005	1.33	44	44	3.5

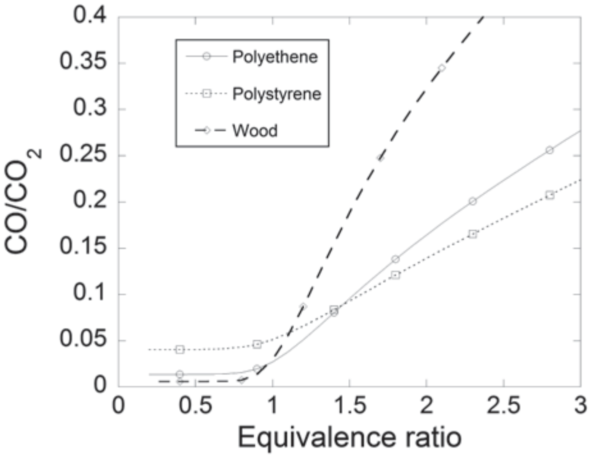

Fig. 7.6 CO/CO_2 ratio for polyethene, polystyrene, and wood as a function of ϕ, based on the work by Tewarson (Eq. (7.16)) [17]

in Fig. 7.6. Polypropene was not included since it is almost identical to polyethene. The curves diverge from each other, but for all three fuels the CO/CO_2 ratio at $\phi = 1$ is between 0.03 and 0.05.

Different fuels utilize available oxygen at high equivalence ratios to very different extents. Beyler [44] reported residual oxygen in exhaust gases from a hood system simulating the upper layer in a two-layer situation at $\phi > 1.2$ for different types of fuels. These results are summarized in Table 7.15. There is a wide range in residual oxygen for the different fuels, from 0.1 % (methanol and ethanol) to 8.0 % (toluene). These values can be compared to the minimum oxygen concentration measured in each test in the Runehamar tunnel: 6.4, 8.6, 11.7, and 15.9 % for T1, T2, T3, and T4, respectively (values corrected for estimated H_2O concentration) [54].

The CO/CO_2 ratio depends on the mode of combustion. For combustion of wood, which is the most common fuel used in large-scale testing in tunnels today, the combustion can be divided into three stages: (1) preflaming pyrolysis, (2) flaming combustion, and (3) char combustion or glowing [58]. Tsuchiya [58] presented mean values of CO/CO_2 ratios for the three phases of combustion for plywood: 0.9

Table 7.15 Residual oxygen for combustion of different fuels at $\phi > 1.2$ [44]

Fuel	Chemical formula	Residual O_2 [%]
Propane	C_3H_8	0.5
Propene	C_3H_6	2.0
Hexanes	C_6H_{14}	3.0
Toluene	C_7H_8	8.0
Methanol	CH_3OH	0.1
Ethanol	C_2H_5OH	0.1
Isopropanol	C_3H_7OH	2.0
Acetone	C_3H_6O	0.7

Table 7.16 CO/CO_2 ratios for selected liquids and noncharforming plastics combusted in normal air in the cone calorimeter [58]

Material	Radiation [kW/m^2]	CO/CO_2
Methanol	5	0.0002
Ethanol	5	0.0004
n-Heptane	5	0.010
Benzene	5	0.065
Xylene	5	0.056
Polypropene	30	0.024
Polypropene	50	0.025
Polystyrene	25	0.046
Polystyrene	40	0.051

(pyrolysis), 0.0035 (flaming combustion), and 0.25 (glowing), respectively. In the discussion above, the mode of combustion has been considered to be flaming in all cases. There is an abrupt transition from preflaming pyrolysis to flaming combustion. Tsuchiya showed that this transition occurred when the O_2 concentration was higher than a certain value that depends on the incident heat flux according to:

$$C_{O_2} = 19.4 - 0.19 \cdot \dot{q}'' \tag{7.17}$$

where C_{O_2} is the concentration of O_2 (in %) and $\dot{q}''$ is the incident heat flux (in kW/m^2).

Modes other than flaming combustion will not be discussed further here. Tsuchiya [58] also presented CO/CO_2 ratios for liquids and noncharring plastics under different levels of incident radiation in the cone calorimeter. Some selected materials of particular interest for the discussion in this section are presented in Table 7.16.

There are large differences between the different types of fuels. When ranking fuels according to their produced CO/CO_2 ratio (from low to high) they can be listed as alcohols and oxygen containing fuels, hydrocarbons, and finally aromatics. This order is valid for well-ventilated conditions. For under ventilated condition the ranking is reversed [60, 44].

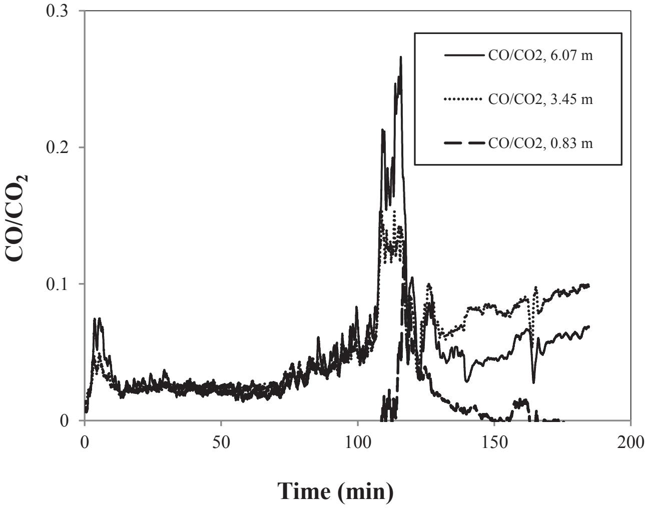

Fig. 7.7 CO/CO_2 ratio at different heights in the tunnel, 100 m downstream of the fire, during test 3 with a commuter train carriage [61]

Lönnermark et al. [61] performed full- scale fire tests with commuter train carriages in a 276 m long tunnel. The concentrations of O_2, CO, and CO_2 were measured at different heights, both in the carriage and in the tunnel. In Fig. 7.7 the CO/CO_2 ratios in the tunnel 100 m downstream of the fire are presented. As can be seen in the figure, the CO/CO_2 ratios clearly exceed the limits discussed above correlating to under ventilated conditions. It was not possible to calculate equivalence ratio in this situation, but this indicates that even if the overall conditions in the tunnel were well-ventilated, the combustion conditions inside the carriage were locally under ventilated. This again illustrates the importance of ventilation conditions on the combustion. The issue of using the CO/CO_2 ratio for determining the ventilation condition is also discussed in Chap. 2.

Example 7.1 A metro carriage is burning in a tunnel. Assume that the fire is locally underventilated with a representative equivalence ratio of $\phi = 1.6$. What would the yields of CO be if the fire could be represented by (1) wood or (2) plastics, for example, polyethene?

Solution:

(1) According to Table 7.14 for wood $y_{CO,\,wv} = 0.005$ *kg/kg,* $\alpha = 44$ *and* $\xi = 3.5$*. Using Eq. (7.15):*

$$y_{CO,wood}(\phi = 1.6) = 0.005 \cdot \left(1 + \frac{44}{e^{2.5 \cdot 1.6^{-3.5}}}\right) = 0.14 \text{ kg/kg}$$

(2) In a similar way for polyethene $y_{CO,\,wv} = 0.024$ *kg/kg,* $\alpha = 10$ *and* $\xi = 2.8$ *and*

$$y_{CO,PE}(\phi = 1.6) = 0.024 \cdot \left(1 + \frac{10}{e^{2.5 \cdot 1.6^{-2.8}}}\right) = 0.38 \text{ kg/kg}$$

To find out the production and concentration of CO both the burning rate (or HRR and combustion efficiency) and air flow in the tunnel need to be known or estimated.

Example 7.2 In a 1.2 km long tunnel, with a width of 9 m and a height of 6 m, an HGV loaded with polypropene is burning in the middle of the tunnel. The fire develops following the "Ultra fast" curve, including a combustion efficiency of 0.9. Estimate the CO/CO_2 ratio after 15 min if the air velocity is 2 m/s and the ambient temperature is 15 °C.

Solution: First the equivalence ratio needs to be calculated. This can be estimated from the HRR according to Eq. (7.12). The fire development can be described as (ultra fast): $\dot{Q} = 0.19 \cdot t^2 = 0.19 \cdot (15 \cdot 60)^2 = 153900 \text{ kW}$. *The mass flow rate can be calculated from:* $\dot{m}_a = \rho_a \cdot u \cdot A = \frac{353}{288} \cdot 2 \cdot 9 \cdot 6 = 132.4 \text{ kg/s}$. *Now Eq. (7.12) gives:* $\phi = \frac{\dot{Q}}{\dot{m}_a \cdot 3000 \cdot \chi} = \frac{153900}{132.4 \cdot 3000 \cdot 0.9} = 0.43$. *The fire is well ventilated. Now, studying Fig. 7.4 and7.6, the* CO/CO_2 *ratio can be estimated to be approximately 0.02. This correlates well also with Table 7.16.*

7.6 Summary

Knowledge of the different species produced during fires is of great importance for estimating the toxicity of the fire smoke. In this chapter the main combustion products from different types of fires are presented. The presentation focuses on CO and the CO/CO_2 ratio, but a large number of species or groups of species are also included, for example, hydrogen chloride (HCl), sulphur dioxide (SO_2), volatile organic compounds (VOCs), polycyclic aromatic hydrocarbons (PAHs), polychlorinated dibenzo-p-dioxins and dibenzofurans (PCDDs/PCDFs), total amount of hydrocarbons (THC) and soot/smoke. The combustion conditions (access of air, temperature, etc.) can vary between different fires in tunnels. Results from measurement during fire tests in vehicles and tunnels are presented in the chapter showing that the ventilation conditions can vary also during the same test leading to very different production rates and yields. The importance of the ventilation conditions on the productions of different species is described and relations for different yields and ratios are given. Especially the relation between the CO/CO_2 ratio and the equivalence ratio is presented and discussed. How to calculate the toxicity when the concentration of a species is known is presented in Chap. 15 on tenability.

References

1. Simonson M, Tuovinen H, Emanuelsson V (2000) Formation of Hydrogen Cyanide in Fires-A Literature and Experimental Investigation. SP Swedish National Testing and Research Institute, Borås, Sweden
2. Purser DA (2000) Toxic product yields and hazard assessment for fully enclosed design fires. Polymer International 49:1232–1255
3. Ferrari LA, Arado MG, Giannuzzi L, Mastrantonio G, Guatelli MA (2001) Hydrogen cyanide and carbon monoxide in blood of convicted dead in a polyurethane combustion: a proposition for the data analysis. Forensic Science International 121:140–143
4. Purser DA (2002) Toxicity Assessment of Combustion Products. In: DiNenno PJ (ed) SFPE Handbook of Fire Protection Engineering. Third Edition edn. National Fire Protection Association, Inc, Quincy, Massachusetts, USA, pp 2–83 -- 82–171
5. Nelson GL (1998) Carbon Monoxide and Fire Toxicity: A Review and Analysis of Recent Work. Fire Technology 34 (1):39–58
6. Gann RG (2004) Sublethal Effects of Fire Smoke. Fire Technology 40:95–99
7. Sader JD, Ou SS (1977) Correlation of the smoke tendency of materials. Fire Research 1 (3)
8. Warnatz J, Maas U, Dibble RW (1996) Combustion-Physical and Chemical Fundamentals, Modeling and Simulation, Experiments, Pollutant Formation. Springer-Verlag, Berlin Heidelberg
9. Glassman I (1996) Combustion. 3rd edn. Academic Press Inc.
10. Atomic Weights of the Elements 1993 (1994). International Union of Pure and Applied Chemistry (IUPAC), Pure & Appl Chem Vol. 66 (No. 12):2423–2444
11. Trends in Atmospheric Carbon Dioxide (2014). Global Greenhouse Gas Reference Network, http://www.esrl.noaa.gov/gmd/ccgg/trends/index.html, Accessed Jan 19. 2014,
12. Weast RC (ed) (1977–78) Handbook of Chemistry and Physics. 58th edn. Chemical Rubber Company
13. Li YZ, Ingason H A new methodology of design fires for train carriages. In: ISTSS 6th International Symposium on Tunnel Safety and Security, Marseille, 2014.
14. Huggett C (1980) Estimation of Rate of Heat Release by Means of Oxygen Consumption Measurements. Fire and Materials 4 (2):61–65
15. Lönnermark A, Stripple H, Blomqvist P (2006) Modellering av emissioner från bränder. SP Sveriges Provnings- och Forskningsinstitut, Borås
16. Persson B, Simonson M, Månsson M (1995) Utsläpp från bränder till atmosfären. SP Sveriges Provnings- och Forskningsinstitut, Borås, Sweden (in Swedish)
17. Tewardson A (2008) Generation of Heat and Gaseous, Liquid, and Solid Products in Fires. In: DiNenno PJ, Drysdale D, Beyler CL et al. (eds) The SFPE Handbook of Fire Protection Engineering. Fourth Edition edn. National Fire Protection Association, Quincy, MA, USA, pp 3–109 -- 103–194
18. ISO (2002) Reaction-to-fire tests-Heat release, smoke production and mass loss rate-Part 1: Heat release rate (cone calorimeter method). 2nd edn. ISO 5660-1
19. Hertzberg T, Blomqvist P, Dalene M, Skarping G (2003) Particles and isocyanates from fires. SP Swedish National Testing and Research Institute, Borås, Sweden
20. Butler K, M., Mulholland GW (2004) Generation and Transport of Smoke Components. Fire Technology 40:149–176
21. Blomqvist P, Persson B, Simonson M (2002) Utsläpp från bränder till miljön-Utsläpp av dioxin, PAH och VOC till luften. Räddningsverket (Swedish Rescue Services Agency), Karlstad, Sweden (in Swedish)
22. Persson B, Simonson M (1998) Fire Emissions into the Atmosphere. Fire Technology 34 (3):266–279
23. Hölemann H Environmental Problems Caused by Fires and Fire-Figthing Agents. In: Fire Safety Science-Proceedings of the Fourth International Symposium, Ottawa, Canada, 13–17 June 1994. International Association for Fire Safety Science (IAFSS), pp 61–77

24. Ahrens M, Rohr KD Fire and the Environment: Issues and Events. In: Proceedings of the Fire Risk and Hazard Assessment Research Application Symposium, Baltimore, Maryland, USA, 9–11 July 2003. The Fire Protection Research Foundation
25. Marlair G, Simonson M, Gann RG Environmental Concerns of Fires: Facts, Figures, Questions and New Challenges for the Future. In: 10th International Fire Science & Engineering Conference (Interflam 2004), Edinburgh, Scotland, 5–7 July 2004. Interscience Communications, pp 325–337
26. Lönnermark A, Blomqvist P (2006) Emissions from an Automobile Fire. Chemosphere 62:1043–1056
27. Fires in Transport Tunnels: Report on Full-Scale Tests (1995). edited by Studiensgesellschaft Stahlanwendung e. V., Düsseldorf, Germany
28. Wichmann H, Lorenz W, Bahadir M (1995) Release of PCDD/F and PAH during Vehicle Fires in Traffic Tunnels. Chemosphere 31 (2):2755–2766
29. Ingason H Heat Release Rate Measurements in Tunnel Fires. In: Ivarson E (ed) International Conference on Fires in Tunnels, Borås, Sweden, October 10–11, 1994 1994. SP Swedish National Testing and Research Institute, pp 86–103
30. Reisman JI (1997) Air Emissions from Scrap Tire Combustion. United States Environmental Protections Agency, EPA-600/R-97-115
31. Lemieux PM, DeMarini D (1992) Mutagenicity of Emissions from the Simulated Open Burning of Scrap Rubber Tires. U.S. Environmental Protection Agency, Control Technology Center, office of Research and Development, EPA-600/R-92-127
32. Lemieux PM, Ryan JV (1993) Characterization of Air Pollutants Emitted from a Simulated Scrap Tire Fire. Journal of the Air & Waste Management Association 43:1106–1115
33. Lemieux PM, Lutes CC, Santoianni DA (2004) Emissions of organic air toxics from open burning: a comprehensive review. Progress in Energy and Combustion Science 30:1–32
34. Conesa JA, Martín-Gullón I, Font R, Jauhiainen J (2004) Complete Study of the Pyrolysis and Gsification of Scrap Tires in a Pilot Plant Reactor. Environmental Science & Technology 38:3189–3194
35. Vianello C, Fabiano B, Palazzi E, Maschio G (2012) Experimental study on thermal and toxic hazards connected to fire scenarios. Journal of Loss Prevention in the Process Industries 25:718–729
36. Ingason H, Lönnermark A, Li YZ (2011) Runehamar Tunnel Fire Tests. SP Technical Research Institute, SP Report 2011:55
37. Ingason H, Lönnermark A (2005) Heat Release Rates from Heavy Goods Vehicle Trailers in Tunnels. Fire Safety Journal 40:646–668
38. Lönnermark A, Ingason H (2005) Gas Temperatures in Heavy Goods Vehicle Fires in Tunnels. Fire Safety Journal 40:506–527
39. Hull TR, Stec AA (2010) Introduction to fire toxicity. In: Stec A, Hull R (eds) Fire Toxicity. CRC
40. Mauring T (2003). Personal communication, Åndalsnes, Norway
41. Nilsen AR, Lindvik PA, Log T Full-scale Fire Testing in Sub Sea Public Road Tunnels. In: Interflam 2001, Edinburgh, Scotland, 17–19 September 2001. Interscience Communications, pp 913–924
42. Ingason H, Bergqvist A, Lönnermark A, Frantzich H, Hasselrot K (2005) Räddningsinsatser i vägtunnlar. Räddningsverket, P21-459/05 (in Swedish)
43. Pitts WM (1994) The Global Equivalence Ratio Concept and the Prediction of Carbon Monoxide Formation in Enclosure Fires. National Institute of Standards and Technology, Gaithersburg, MD, USA
44. Beyler CL (1986) Major Species Production by Diffusion Flames in a Two-layer Compartment Fire Environment. Fire Safety Journal 10:47–56
45. Gottuk DT (1992) Carbon Monoxide Production in Compartment Fires. Journal of Fire Protection Engineering 4 (4):133–150

46. Gottuk DT, Lattimer BY (2002) Effect of Combustion Conditions on Species Production. In: DiNenno PJ (ed) SFPE Handbook of Fire Protection Engineering. Third Edition edn. National Fire Protection Association, Inc, Quincy, Massachusetts, USA, pp 2–54 -- 52–82
47. Blomqvist P, Lönnermark A (2001) Characterization of the Combustion Products in Large-scale Fire Tests: Comparison of Three Experimental Configurations. Fire and Materials 25:71–81
48. Babrauskas V, Parker WJ, Mulholland G, Twilley WH (1994) The phi meter: A simple, fuel-independent instrument for monitoring combustion equivalence ratio. Rev Sci Instrum 65 (7):2367–2375
49. Lönnermark A, Babrauskas V (1997) TOXFIRE-Fire Characteristics and Smoke Gas Analyses in Under-ventilated Large-scale Combustion Experiments: Theoretical Background and Calculations. SP Swedish National Testing and Research Institute, Borås, Sweden
50. Ingason H Fire Development in Catastrophic Tunnel Fires (CTF). In: Ingason H (ed) International Symposium on Catastrophic Tunnel Fires (CTF), Borås, Sweden, 20–21 November 2003. SP Swedish National Testing and Research Institute, pp 31–47
51. Ingason H (1995) Effects of Ventilation on Heat Release Rate of Pool Fires in a Model Tunnel. SP Swedish National Testing and Research Institute, Borås, Sweden
52. Ingason H (1995) Fire Experiments in a Model Tunnel using Pool Fires-Experimental Data. SP Swedish National Testing and Research Institute, Borås, Sweden
53. Lönnermark A, Blomqvist P, Månsson M, Persson H (1997) TOXFIRE-Fire Characteristics and Smoke Gas Analysis in Under-ventilated Large-scale Combustion Experiments: Tests in the ISO 9705 Room. SP Swedish National Testing and Research Institute, Borås, Sweden
54. Lönnermark A (2005) On the Characteristics of Fires in Tunnels. Doctoral Thesis, Doctoral thesis, Department of Fire Safety Engineering, Lund University, Lund, Sweden
55. Ingason H (2005) Fire Dynamics in Tunnels. In: Carvel RO, Beard AN (eds) The Handbook of Tunnel Fire Safety. Thomas Telford Publishing, London, pp 231–266
56. Grant GB, Drysdale D Estimating Heat Release Rates from Large-scale Tunnel Fires. In: Fire Safety Science-Proceedings of the Fifth International Symposium, Melbourne, 1995. pp 1213–1224
57. Gottuk DT, Roby RJ, Beyler CL (1995) The Role of Temperature on Carbon Monoxide Production in Compartment Fires. Fire Safety Journal 24:315–331
58. Tsuchiya Y CO/CO_2 Ratios in Fire. In: Fire Safety Science-Proceedings of the Fourth International Symposium, Ottawa, Canada, 13–17 June 1994. IAFSS, pp 515–526
59. Bettis RJ, Jagger SF, Wu Y (1993) Interim Validation of Tunnel Fire Consequence Models: Summary of Phase 2 Tests. Health and Safety Executive, Buxton, Derbyshire, UK
60. Beyler CL Major Species Production by Solid Fuels in a Two Layer Compartment Fire Environment. In: Fire Safety Science-Proceedings of the First International Symposium, Gaithersburg, USA, 7–11 October 1985. IAFSS, pp 431–440
61. Lönnermark A, Claesson A, Lindström J, Li YZ, Kumm M, Ingason H Gas composition during a fire in a train carriage. In: Proceedings from the Sixth International Symposium on Tunnel Safety and Security (ISTSS 2014), Marseille, France, 12–14 March 2014. SP Technical Research Institute of Sweden